Theory of spontaneous emission of quantum dots in the linear regime

2007 J. Phys.: Condens. Matter 19 406201

(http://iopscience.iop.org/0953-8984/19/40/406201)

IOP PUBLISHING JOURNAL OF PHYSICS: CONDENSED MATTER

J. Phys.: Condens. Matter **19** (2007) 406201 (9pp) doi:10.1088/0953-8984/19/40/406201

Theory of spontaneous emission of quantum dots in the linear regime

A Zora[1], C Simserides[1,2] and G P Triberis[1]

[1] Physics Department, University of Athens, Panepistimiopolis, Zografos, GR-15784, Athens, Greece
[2] Materials Science Department, University of Patras, Panepistimiopolis, Rio, GR-26504, Patras, Greece

E-mail: gtriber@phys.uoa.gr

Received 6 March 2007, in final form 3 August 2007
Published 11 September 2007
Online at stacks.iop.org/JPhysCM/19/406201

Abstract

We develop a fully quantum-mechanical theory for the interaction of light and electron–hole excitations in semiconductor quantum dots. Our theoretical analysis results in an expression for the photoluminescence intensity of quantum dots in the linear regime. Taking into account the single-particle Hamiltonian, the free-photon Hamiltonian, the electron–hole interaction Hamiltonian, and the interaction of carriers with light, and applying the Heisenberg equation of motion to the photon number expectation values, to the carrier distribution functions and to the correlation term between the photon generation (destruction) and electron–hole pair, we obtain a set of luminescence equations. Under quasi-equilibrium conditions, these equations become a closed-set of equations. We solve them analytically, in the linear regime, and we find an approximate solution of the incoherent photoluminescence intensity. The validity of the theoretical analysis is tested by investigating the emission spectra in the high-temperature regime, interpreting the experimental findings for the emission spectra of a lens-shaped $In_{0.5}Ga_{0.5}As$ self-assembled quantum dot. Our theoretical predictions for the interlevel spacing as well as for the dephasing time caused by electron–longitudinal optical phonon interactions are in good agreement with the experimental results.

1. Introduction

Semiconductor quantum dots (QDs) will be at the core of several technologies such as quantum dot based lasers or quantum information for many years. Among the QDs fabricated by various techniques, self-assembled QDs have excellent optical quality and are most suitable for the photonic device fabrication owing to the capability of their high-density growth. A great effort has been devoted to the understanding of the conditions that affect their size, shape, density and

spatial arrangements. Recent experimental studies [1] pointed out that the shapes and therefore the optical properties of QDs grown by the Stranski–Krastanov (SK) technique depend strongly on the orientation (high-index planes) and on the growth conditions, such as the capping process or the growth interruption.

Photoluminescence (PL) is a powerful tool for the understanding of the QDs characteristics and it has been intensively studied in recent years both experimentally [2–5] and theoretically [6–10].

In this paper we develop a theory for the spontaneous emission of individual quantum dots or quantum dot molecules, taking into account the interaction of the electron–hole excitations with light. Kira *et al* [11, 12] developed a microscopic theory for the spontaneous emission in quantum wells a few years ago. On the other hand, near-field spectroscopy [13, 14] seems to be ideally suited to investigating the properties of individual quantum dots within a dot ensemble realized in a realistic structure. Here, we discuss the purely incoherent photoluminescence resulting from the recombination of the excited electrons and holes. The situations in which coherent sources resonantly excite the quantum dot and a classical driving field must be included are beyond the scope of this analysis.

Assuming that the total Hamiltonian of the system consists of the single-particle Hamiltonian, the free-photon Hamiltonian, the electron–hole interaction Hamiltonian, and the Hamiltonian that expresses the interaction of carriers with light, and applying the Heisenberg equation of motion to the photon number expectation values, to the carrier distribution functions $f^{\mu e}$, $f^{\nu h}$ and to the correlation term between the photon generation or destruction and electron–hole pair destruction or generation, we obtain a set of luminescence equations. Under incoherent [15] and quasi-equilibrium conditions, i.e., for given carrier densities, we obtain a closed set of equations. Solving these equations analytically, in the linear regime ($1 - f^{\mu e} - f^{\nu h} \approx 1$), we find an approximate solution of the photoluminescence intensity.

Matsuda *et al* [13] investigated the PL properties of single self-assembled $In_{0.5}Ga_{0.5}As$ quantum dots, using a highly sensitive near-field scanning optical microscope at room temperature. By employing an optimized fiber probe having a high collection efficiency and a high spatial resolution, weak PL signals from single quantum dots were collected. Therefore, we have decided to test our theoretically calculated emission spectra for single QDs with the experimental PL data of an individual lens-shaped self-assembled QD reported therein [13]. Our theoretical predictions for the interlevel spacing [13] as well as for the dephasing time caused by electron–longitudinal optical (LO) phonon interactions [16–19] are in good agreement with the experimental results.

2. The physical system

The physical system can be described by the following Hamiltonian:

$$H = H_{\mathrm{sp}} + H_{\gamma} + H_{\mathrm{cc}} + H_{\mathrm{c}\gamma}. \tag{1}$$

The first term describes the single-particle system in the presence of an external electric or magnetic static field, while the second term refers to the free-photon system. H_{cc} and $H_{\mathrm{c}\gamma}$ stand for the carrier–carrier interaction and interaction of the carrier with the background photon field [20]. The fist three terms of the Hamiltonian are generally given by [21]. In order to discuss their explicit form in quantum dots, we introduce the usual second-quantization field operators in the electron–hole picture,

$$\begin{aligned} \Psi^{\dagger}(\mathbf{r}, t) &= \sum_{\mu} c_{\mu}^{\dagger}(t)\Phi^{\mu e*}(\mathbf{r}) + \sum_{\nu} d_{\nu}(t)\Phi^{\nu h}(\mathbf{r}) \\ \Psi(\mathbf{r}, t) &= \sum_{\mu} c_{\mu}(t)\Phi^{\mu e}(\mathbf{r}) + \sum_{\nu} d_{\nu}^{\dagger}(t)\Phi^{\nu h*}(\mathbf{r}). \end{aligned} \tag{2}$$

$\Phi^{\mu e}$ and $\Phi^{\nu h}$ are the single-particle envelope functions [23], and μe (νh) denotes the different electron (hole) states. Also, $c^{\dagger}_{\mu}$ and $d^{\dagger}_{\nu}$ are the electron and hole creation operators respectively.

The Hamiltonian of the non-interacting carriers confined in the quantum dot and subjected to an external magnetic field is generally given by [21]

$$H_{\rm sp} = \int {\rm d}\mathbf{r}\, \hat{\mathbf{\Psi}}^{\dagger}(\mathbf{r},t) \left[\frac{(-{\rm i}\hbar\nabla_{\mathbf{r}} - \frac{e}{c}\mathbf{A}(\mathbf{r},t))^2}{2m^*} + e\phi(\mathbf{r},t) + V(\mathbf{r}) \right] \hat{\mathbf{\Psi}}(\mathbf{r},t) \quad (3)$$

where $V(\mathbf{r})$ is the three-dimensional quantum dot confining potential and $\mathbf{A}(\mathbf{r},t)$, $\phi(\mathbf{r},t)$, the vector and scalar potentials of the external magnetic field. Inserting the second-quantization field operators to the single-particle Hamiltonian we get

$$H_{\rm sp} = \sum_{\mu\mu'} E^{\rm e}_{\mu\mu'} c^{\dagger}_{\mu}(t) c_{\mu'}(t) + \sum_{\nu\nu'} E^{\rm h}_{\nu\nu'} d^{\dagger}_{\nu}(t) d_{\nu'}(t), \quad (4)$$

where the matrix elements [21] of the above Hamiltonian are

$$\begin{aligned} E^{\rm e}_{\mu\mu'} &= \int {\rm d}\mathbf{r}\, \Phi^{\mu e*}(\mathbf{r}) \left[\frac{(-{\rm i}\hbar\nabla_{\mathbf{r}} - \frac{e}{c}\mathbf{A}(\mathbf{r},t))^2}{2m^*} + e\phi(\mathbf{r},t) + V(\mathbf{r}) \right] \Phi^{\mu' e}(\mathbf{r}) \\ E^{\rm h}_{\nu\nu'} &= -\int {\rm d}\mathbf{r}\, \Phi^{\nu h*}(\mathbf{r}) \left[\frac{(-{\rm i}\hbar\nabla_{\mathbf{r}} - \frac{e}{c}\mathbf{A}(\mathbf{r},t))^2}{2m^*} + e\phi(\mathbf{r},t) + V(\mathbf{r}) \right] \Phi^{\nu' h}. \end{aligned} \quad (5)$$

Since our single-particle eigenfunctions are constructed to be orthonormal, the single-particle Hamiltonian is finally written as

$$H_{\rm sp} = \sum_{\mu} E^{\mu e} c^{\dagger}_{\mu}(t) c_{\mu}(t) + \sum_{\nu} E^{\nu h} d^{\dagger}_{\nu}(t) d_{\nu}(t) = H_{\rm se} + H_{\rm sh}. \quad (6)$$

$E^{\mu e}$ and $E^{\nu h}$ are the electron and hole eigenenergies.

The free-photon Hamiltonian is given by

$$H_{\gamma} = \sum_{q} \hbar\omega_q \alpha^{\dagger}_q(t) \alpha_q(t), \quad (7)$$

where $a^{\dagger}_q$ (a_q) is the creation (destruction) nonlocal bosonic photon operator, and $\hbar\omega_q$ is the photon energy.

The carrier–carrier interaction is described by the two-body Hamiltonian [21],

$$H_{\rm cc} = \tfrac{1}{2} \int {\rm d}\mathbf{r} \int {\rm d}\mathbf{r}'\, \hat{\mathbf{\Psi}}^{\dagger}(\mathbf{r},t) \hat{\mathbf{\Psi}}^{\dagger}(\mathbf{r}',t) V^{\rm cc}(\mathbf{r}-\mathbf{r}') \hat{\mathbf{\Psi}}(\mathbf{r}',t) \hat{\mathbf{\Psi}}(\mathbf{r},t). \quad (8)$$

Inserting the second-quantization field operators and neglecting terms that do not conserve the number of electron–hole pairs, such as Auger recombination and impact ionization [22], as well as terms that refer to interband exchange interaction, we finally get

$$\begin{aligned} H_{\rm cc} = {} & \tfrac{1}{2} \sum_{\mu_1\mu_2\mu_3\mu_4} V^{\rm ee}_{\mu_1\mu_2\mu_3\mu_4} c^{\dagger}_{\mu_1} c^{\dagger}_{\mu_2} c_{\mu_3} c_{\mu_4} + \tfrac{1}{2} \sum_{\nu_1\nu_2\nu_3\nu_4} V^{\rm hh}_{\nu_1\nu_2\nu_3\nu_4} d^{\dagger}_{\nu_1} d^{\dagger}_{\nu_2} d_{\nu_3} d\nu_4 \\ & - \sum_{\mu_1\mu_2\nu_1\nu_2} V^{\rm eh}_{\mu_1\nu_1\nu_2\mu_2} c^{\dagger}_{\mu_1} d^{\dagger}_{\nu_1} d_{\nu_2} c_{\mu_2} = H_{\rm ee} + H_{\rm hh} + H_{\rm eh}. \end{aligned} \quad (9)$$

The Coulomb matrix elements have been determined in [23].

$$V^{\rm cc}_{\kappa_1\kappa_2\kappa_3\kappa_4} \equiv \int {\rm d}\mathbf{r} \int {\rm d}\mathbf{r}' \Phi^{\kappa_1 *}(\mathbf{r}) \Phi^{\kappa_2 *}(\mathbf{r}') V^{\rm cc}(\mathbf{r}-\mathbf{r}') \Phi^{\kappa_3}(\mathbf{r}') \Phi^{\kappa_4}(\mathbf{r}). \quad (10)$$

The Hamiltonian $H_{c\gamma}$ is obtained when the light field is treated quantum mechanically [20, 24], and within our notation is expressed by

$$\begin{aligned} H_{c\gamma} = {} & \mathbf{A}_0^{1/2} {\rm i} \sum_{q\mu\nu} \omega_q^{1/2} [\mathbf{M}^*_{\mu\nu} \alpha^{\dagger}_q(t) d_{\nu}(t) c_{\mu}(t) - \mathbf{M}_{\mu\nu} \alpha_q(t) c^{\dagger}_{\mu}(t) d^{\dagger}_{\nu}(t) \\ & - \mathbf{M}_{\mu\nu} \alpha^{\dagger}_q(t) c^{\dagger}_{\mu}(t) d^{\dagger}_{\nu}(t) + \mathbf{M}^*_{\mu\nu} \alpha_q(t) d_{\nu}(t) c_{\mu}(t)]. \end{aligned} \quad (11)$$

Here, $\mathbf{M}_{\mu\nu} = e\int \Phi^{\mu e*}(\mathbf{r})\mathbf{r}\Phi^{\nu h*}(\mathbf{r})$ are the total dipole matrix elements [25] and $\mathbf{A_0}$ is the amplitude of the vector potential of the photon field.

Our kinetic description is based on the density matrix formalism. We consider the operator

$$\wp_{\mu\nu}(t) = d_\nu(t)c_\mu(t), \tag{12}$$

the expectation value of which gives the microscopic (optical) polarization of the system. We also consider the intraband electron and hole single-particle density matrices

$$\begin{aligned}\hat{n}_{\mu\mu'} &= c^\dagger_\mu c_{\mu'}\\ \hat{n}_{\nu\nu'} &= d^\dagger_\nu d_{\nu'}.\end{aligned} \tag{13}$$

The expectation values of the diagonal elements correspond to electron and hole distribution functions $f^{\mu e}$ and $f^{\nu h}$.

3. The luminescence equations

We apply the Heisenberg equation of motion to the photon number expectation values $\langle a^\dagger_q a_{q'}\rangle$ and to the field–matter correlations of the type $\langle a^\dagger_q \wp_{\mu\nu}\rangle \equiv \langle a^\dagger_q d_\nu c_\mu\rangle$, and we obtain a set of luminescence equations. The dynamics for the expectation values of $\wp_{\mu\nu}$ and $\hat{n}_{\mu\mu'}$ (or $\hat{n}_{\nu\nu'}$) is partly determined by combinations of four-carrier operators due to the Coulomb interaction as well as by a mixture of one-photon and two-carrier operators as a result of the quantized light–matter interaction. For the decoupling of the above combinations we use the semiclassical Hartree–Fock scheme. Since the Hartree–Fock level does not anticipate the influence of dephasing [12], we will include this effect phenomenologically through a small damping constant γ, which in the relaxation time approximation is related to the dephasing time $\tau = \frac{\hbar}{\gamma}$. We focus on the theoretical analysis of incoherent luminescence, where shortly after an optical excitation of the carriers high above the dot discrete states non-resonant with the bound excitonic states, all coherent polarizations dephase.

In the specific case of very small electron and hole distribution functions $f^{\mu e/\nu h}$, i.e., in the linear regime where $1 - f^{\mu e} - f^{\nu h} \approx 1$, we can neglect the renormalization term of the single-particle energies [20], and the three luminescence equations become

$$\mathrm{i}\hbar\frac{\partial\langle a^\dagger_q a_{q'}\rangle}{\partial t} = \hbar(\omega_{q'} - \omega_q)\langle a^\dagger_q a_{q'}\rangle + \mathrm{i}\mathbf{A_0}^{1/2}\sum_{\mu\nu}[\mathbf{M}^*_{\mu\nu}\omega^{1/2}_{q'}\langle a^\dagger_q \wp_{\mu\nu}\rangle + \mathbf{M}_{\mu\nu}\omega^{1/2}_q\langle a_{q'}\wp^\dagger_{\mu\nu}\rangle], \tag{14}$$

$$\begin{aligned}\mathrm{i}\hbar\frac{\partial\langle a^\dagger_q \wp_{\mu\nu}\rangle}{\partial t} &= (E^{\mu e} + E^{\nu h} - \hbar\omega_q)\langle a^\dagger_q \wp_{\mu\nu}\rangle - \mathbf{M}_{\mu\nu}\sum_{q'}\mathrm{i}\mathbf{A_0}^{1/2}\omega^{1/2}_{q'}\langle a^\dagger_q a_{q'}\rangle\\ &\quad - \sum_{\mu'\nu'} V^{\mathrm{eh}}_{\mu\mu',\nu\nu'}\langle a^\dagger_q \wp_{\mu'\nu'}\rangle + \mathrm{i}f^{\mu e}f^{\nu h}\mathbf{M}_{\mu\nu}\mathbf{A_0}^{1/2}\omega^{1/2}_q,\end{aligned} \tag{15}$$

and

$$\mathrm{i}\hbar\frac{\partial f^{\mu e}}{\partial t} = 2\mathrm{i}\mathbf{A}^{1/2}_0\sum_{q\nu}\omega^{1/2}_q\,\mathrm{Im}[-\mathrm{i}\mathbf{M}^*_{\mu\nu}\langle\alpha^\dagger_q\wp_{\mu\nu}\rangle]. \tag{16}$$

For given carrier densities, i.e., under quasi-equilibrium conditions, the above set of equations is restricted to the closed set of equations (14) and (15).

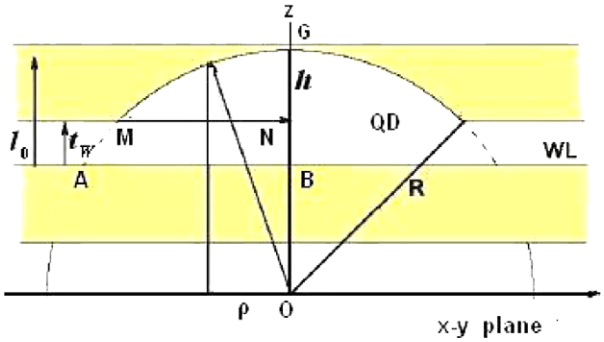

Figure 1. Cross-sectional view of an ideal lens-shaped QD [29, 31]. (AB) $= \rho_0$, (MN) $= s$ the radius at the base, and (GN) $= h$ the height of the dot.

(This figure is in colour only in the electronic version)

4. The QD photoluminescence intensity

We make the assumption that the pure stimulated term analogous to $\langle a_q^\dagger a_{q'}\rangle$ is artificially switched off. Using the notation $\ell \equiv \mu\nu$, equation (15) becomes

$$\mathrm{i}\hbar\frac{\partial}{\partial t}\langle\alpha_q^\dagger(t)\wp_\ell(t)\rangle = \sum_{\ell'}(S_{\ell\ell'} - \hbar\omega_q\delta_{\ell\ell'})\langle\alpha_q^\dagger\wp_{\ell'}\rangle + \mathrm{i}f^{\mu\mathrm{e}}f^{\nu\mathrm{h}}\mathbf{A}_0^{1/2}\omega_q^{1/2}\mathbf{M}_\ell. \tag{17}$$

$S_{\ell\ell'} \equiv T_\ell\delta_{\ell\ell'} - V_{\ell\ell'}^{\mathrm{eh}}$ is the excitonic matrix [23], which is Hermitian in our regime of interest, and

$$T_\ell \equiv E^{\mu\mathrm{e}} + E^{\nu\mathrm{h}} \tag{18}$$

the summation of the single-particle energies. In appendix B we solve analytically the closed set of equations (14) and (17) and find an approximate solution of the photoluminescence intensity ($I_{\mathrm{em}}(\omega_q) \equiv \frac{\partial}{\partial t}\langle a_q^\dagger a_q\rangle$)

$$I_{\mathrm{em}}(\omega_q) \propto \mathrm{Im}\sum_\lambda\left[\frac{1}{(E^\lambda - \hbar\omega_q - \mathrm{i}\gamma)}\int \mathrm{d}\mathbf{r}\,\Psi^\lambda(\mathbf{r},\mathbf{r})\int \mathrm{d}\mathbf{r}\sum_\ell \mathcal{C}_\ell^{\lambda *}\Phi^{\mu\mathrm{e}*}(\mathbf{r})\Phi^{\nu\mathrm{h}*}(\mathbf{r})f^{\mu\mathrm{e}}f^{\nu\mathrm{h}}\right]. \tag{19}$$

$\Psi^\lambda(\mathbf{r},\mathbf{r})$ is the excitonic eigenfunction which is expanded in terms of the single-particle states [23]. In the high-temperature regime the carrier occupation probabilities are given by the Fermi–Dirac distribution functions [26]. The above formula for the PL intensity can be applied to single or double quantum dots of any given geometry and under a magnetic field of any magnitude and orientation.

5. Comparison with experiment

We use our theoretical results to interpret the experimental findings reported by Matsuda *et al* [13]. The real geometry of self-assembled In(Ga)As quantum dots grown on GaAs substrates is rather complicated. For example, Kiravittaya *et al* [27] reported two types of QD shapes: pyramids elongated along the [1-10] directions bounded by [137] facets, and domes with a multi-faceted shape. However, we approximate the specific $In_{0.5}Ga_{0.5}As$ self-assembled quantum dot with a lens-shaped potential (figure 1). s is the radius at the base and $h =$ (GN) the height of the quantum dot. The thickness of the wetting layer (WL) is $t_{\mathrm{W}} = 4$ ML [13],

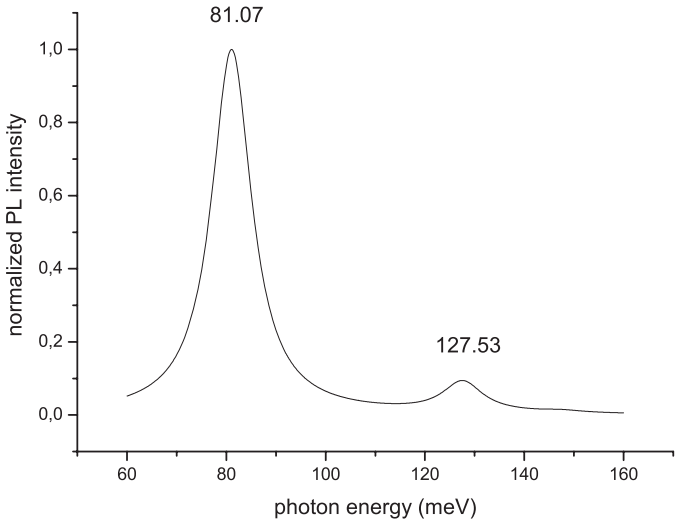

Figure 2. The room-temperature emission spectra of a single $In_{0.5}Ga_{0.5}As$ lens-shaped self-assembled quantum dot with diameter at the base 33.6 nm and height 9.5 nm. The photon energy, $\hbar\omega_q$ (meV), is measured with respect to the band gap.

which according to the values reported [28], equals 1.1 nm. As shown in figure 1, a quantum well of thickness $l_0 = h + t_W$ can become a lens-shaped quantum dot of similar total thickness at the center and radius $\rho_0 = l_0\sqrt{1 + \frac{s^2-h^2-2t_w h}{hl_0}}$.

In the III–V semiconductor material system, the SK process allows for the formation of InAs islands on GaAs and it has been shown that the small dots and surrounding host matrix are dislocation free and strained coherently with GaAs [1]. So, we can approximate the strained $In_{0.5}Ga_{0.5}As$ material in the dot by just taking the bulk GaAs effective mass value [28]. Moreover, for strained $In_xGa_{1-x}As$ one expects the mixing between light and heavy holes to be small, and we therefore approximate the hole energy levels in the same way as for an electron [29] (i.e., one band approximation) but with a different effective mass and depth of confining potential. The electron (hole) effective mass is $0.0632m_e$ ($0.11m_e$) [30], where m_e is the electron mass. For the conduction-band and valence-band offsets we take $\Delta V_{CB} = 224$ meV and $\Delta V_{VB} = 180$ meV, respectively. We calculate the single-particle eigenstates of electrons and holes within the effective mass and envelope function approximations [23]. Using an expansion—within a periodicity box—of the electron (or hole) envelope functions into the orthonormal plane-wave basis $|\Phi^\mu\rangle = \sum_{\mathbf{k}} C^\mu_{\mathbf{k}}|\mathbf{k}\rangle$ [23], we obtain the eigenenergies E^μ as well as $C^\mu_{\mathbf{k}}$ by full three-dimensional (3D) numerical diagonalization; i.e., we solve the following eigenvalue problem:

$$\sum_{\mathbf{k}'}\left[\langle\mathbf{k}|\left(\frac{\mathbf{p}^2}{2m^*} + V(\mathbf{r})\right)|\mathbf{k}'\rangle - E^\mu\delta_{\mathbf{k},\mathbf{k}'}\right]\langle\mathbf{k}'|\Phi^\mu\rangle = 0. \tag{20}$$

The 3D confining potential is zero inside the wetting layer and the self-assembled dot, and ΔV_{CB} (or ΔV_{VB}) inside the barrier. The single-particle eigenfunctions have cylindrical symmetry and resemble the Darwin–Fock states [32, 33]. The details of the theoretical steps of the calculation of the excitonic eigenfunctions have already been presented in detail [23].

Our theoretical results for the PL intensity are presented in figure 2. All energies are given with respect to the band gap. We observe two features: the first one at 81.1 meV is

exclusively composed of the ground-state transition, i.e., from 1s(e) to 1s(h). The second feature at 127.8 meV is mainly composed of the following transitions: from 1s(e) to 2s(h), and 1p(e) to 1p(h).

Using $s = 16.8$ and $h = 9.5$ nm, values which are within the range of the values reported by Matsuda *et al* [13], for the size distribution of the QDs, we reproduce the exact value of the experimental interlevel spacing $\Delta E = 47$ meV [13]. If the position of the first feature corresponds to the value 1158 meV reported [13], our theoretical approach results in a value 1077 meV for the band gap, which is close to $E_g = 1019$ meV reported [30]. Finally, in order to obtain the experimental full width at half maximum (FWHM) of ≈ 10 meV, we take $\gamma = 4.9$ meV. This value leads to $\tau = 130$ fs, which is in good agreement with values of the LO phonon dephasing times reported both in experimental [16–18] and in theoretical studies [19], where the dephasing of optical transitions in QDs has been attributed to second-order elastic (i.e., without changing the populations of the carrier energy levels) interaction with LO phonons.

Our theoretical approach for the emission spectra of quantum dots explains satisfactorily the experimental data reported for the PL spectra collected with a high spatial resolution near-field microscope. Additionally, it allows the determination of the interlevel spacing as well as the LO phonon dephasing time.

Acknowledgment

This work was supported by the Hellenic Ministry of Education under the program *Heracletus*.

Appendix A. The semiclassical equation of the optical polarization

Since there is no coherent field and intraband polarization, the initial values are

$$\begin{aligned} &p_{\mu\nu} \equiv \langle \wp_{\mu\nu}(t = t_0)\rangle = 0 \\ &\langle a_q(t = t_0)\rangle = 0. \end{aligned} \tag{A.1}$$

Using the Heisenberg equation of motion for the microscopic polarization, taking the system just after the excitation, we obtain

$$\begin{aligned} \frac{\partial p_{\mu\nu}}{\partial t} = \frac{1}{\mathrm{i}\hbar}\sum_{\mu'\nu'}(E^{\mathrm{e,renorm}}_{\mu\mu'}\delta_{\nu\nu'} + E^{\mathrm{h,renorm}}_{\nu\nu'}\delta_{\mu\mu'})p_{\mu'\nu'} \\ - \frac{1}{\mathrm{i}\hbar}\sum_{\mu'\nu'} V^{\mathrm{eh}}_{\mu\nu\nu'\mu'}p_{\mu'\nu'}(1 - f^{\mu\mathrm{e}} - f^{\nu\mathrm{h}}) \end{aligned} \tag{A.2}$$

where

$$E^{\mathrm{e/h,renorm}}_{\kappa_1\kappa_2} = E_{\kappa_1}\delta_{\kappa_1\kappa_2} - \sum_{\kappa_3} V^{\mathrm{ee/hh}}_{\kappa_1\kappa_3\kappa_2\kappa_3} f^{\kappa_3,\mathrm{e/h}} \tag{A.3}$$

are the renormalized single-particle energies. The optical polarization in the excitonic picture is given by

$$p^{\lambda}(t) = \sum_{\ell} C^{\lambda *}_{\ell} p_{\ell}(t). \tag{A.4}$$

Inserting (A.4), we can rewrite equation (A.2) in the excitonic picture as

$$\frac{\partial p^{\lambda}}{\partial t} = \frac{1}{\mathrm{i}\hbar}E^{\lambda}p^{\lambda}(t). \tag{A.5}$$

Taking the Fourier transformation of the above equation we have

$$(E^{\lambda} - \hbar\omega)p^{\lambda}(\omega) = 0. \tag{A.6}$$

It is obvious that in the vicinity of the excitonic resonances $p^{\lambda}(\omega) = 0$, and therefore $p_{\ell}(t > t_0) = 0$.

$$p_{\mu\nu} \equiv \langle \wp_{\mu\nu}(t) \rangle = 0. \tag{A.7}$$

So, the only nonzero quantities are $f^{\mu e}$, $f^{\nu h}$, $\langle \alpha_q^{\dagger}(t)\alpha_{q'}(t)\rangle$ and $\langle \alpha_q^{\dagger}(t)\wp_{\mu\nu}(t)\rangle$.

Appendix B. Analytical solution of the QD luminescence equations

The eigenvalue equation for the matrix $\hat{S}$ is [23]

$$\sum_{\ell} C_{\ell}^{\lambda *} S_{\ell\ell'} = E^{\lambda} C_{\ell'}^{\lambda *} \tag{B.1}$$

The eigenvector components C_{ℓ}^{λ} are the matrix elements of the unitary transformation connecting the original non-interacting basis $|eh\rangle$ with the excitonic basis $|\lambda\rangle$, i.e., $C_{\ell'}^{\lambda} = \langle \ell|\lambda\rangle$. The E^{λ} are the excitonic eigenvalues in the linear regime. Is is obvious that the matrix $\hat{R}$ with elements $R_{\ell\ell'} \equiv S_{\ell\ell'} - \hbar\omega\delta_{\ell\ell'}$ has the same eigenvectors as the excitonic matrix, and eigenvalues equal to $E^{\lambda} - \hbar\omega$. Setting $Q_{\ell} = \langle \alpha_q^{\dagger}(t)\wp_{\ell}(t)\rangle$ for the correlation term, the steady-state solution follows from the equation:

$$\begin{aligned}
&\sum_{\ell'} R_{\ell\ell'} Q_{\ell'} = -\mathrm{i}\mathbf{A}_0^{1/2}\omega_q^{1/2} f^{\mu e} f^{\nu h}\mathbf{M}_{\ell} \Leftrightarrow \\
&\sum_{\ell'}\left[\sum_{\ell} C_{\ell}^{\lambda *} R_{\ell\ell'}\right] Q_{\ell'} = -\mathrm{i}\mathbf{A}_0^{1/2}\omega_q^{1/2}\sum_{\ell}\mathbf{M}_{\ell} f^{\mu e} f^{\nu h} C_{\ell}^{\lambda *} \Leftrightarrow \\
&(E^{\lambda} - \hbar\omega)\left[\sum_{\ell'} C_{\ell'}^{\lambda *} Q_{\ell'}\right] = -\mathrm{i}\mathbf{A}_0^{1/2}\omega_q^{1/2}\sum_{\ell}\mathbf{M}_{\ell} f^{\mu e} f^{\nu h} C_{\ell}^{\lambda *}.
\end{aligned} \tag{B.2}$$

By applying this unitary transformation we can rewrite equation (B.2) in the excitonic picture,

$$Q^{\lambda} = \frac{-\mathrm{i}\mathbf{A}_0^{1/2}\omega_q^{1/2}\sum_{\ell}\mathbf{M}_{\ell} f^{\mu e} f^{\nu h} C_{\ell}^{\lambda *}}{E^{\lambda} - \hbar\omega}, \tag{B.3}$$

where

$$Q^{\lambda} \equiv \sum_{\ell'} C_{\ell'}^{\lambda *} Q_{\ell'} \tag{B.4}$$

denotes the correlation term in the excitonic picture. Using the excitonic function orthogonality relation, i.e., $\sum_{\lambda} C_{\ell}^{\lambda} C_{\ell'}^{\lambda *} = \delta_{\ell\ell'}$, the first PL equation (14) can be rewritten for $\mathbf{q} = \mathbf{q}'$ as

$$\frac{\partial}{\partial t}\langle \alpha_q^{\dagger}\alpha_q\rangle = \frac{\mathbf{A}_0^{1/2}\omega_q^{1/2}}{\hbar}\sum_{\lambda}\left[\sum_{\ell'}\sum_{\ell}\mathbf{M}_{\ell}^{*} C_{\ell}^{\lambda} Q_{\ell'} C_{\ell'}^{\lambda *} + \sum_{\ell'}\sum_{\ell}\mathbf{M}_{\ell'} C_{\ell'}^{\lambda *} Q_{\ell}^{*} C_{\ell}^{\lambda}\right]. \tag{B.5}$$

Due to the definition of the dipole matrix elements in the excitonic picture, ($\mathbf{M}^{\lambda}(\mathbf{r}) = \sum_{\ell} C_{\ell}^{\lambda *}\mathbf{M}_{\ell}(\mathbf{r})$), and the correlation term as well, the time evolution of the expectation value of the number of the photons can be written as

$$\frac{\partial}{\partial t}\langle \alpha_q^\dagger \alpha_q \rangle = \frac{\mathbf{A}_0^{1/2}\omega_q^{1/2}}{\hbar}\sum_\lambda (Q^\lambda \mathbf{M}^{\lambda *} + Q^{\lambda *}\mathbf{M}^\lambda)$$
$$= \frac{\mathbf{A}_0^{1/2}\omega_q^{1/2}}{\hbar}\sum_\lambda \left(\frac{\mathbf{M}^{\lambda *}(-\mathrm{i})\mathbf{A}_0^{1/2}\omega_q^{1/2}\sum_\ell \mathbf{M}_\ell f^{\mu \mathrm{e}} f^{\nu \mathrm{h}} C_\ell^{\lambda *}}{E^\lambda - \hbar\omega} \right.$$
$$\left. + \frac{\mathbf{M}^\lambda \mathrm{i}\mathbf{A}_0^{1/2}\omega_q^{1/2}\sum_\ell C_\ell^\lambda \mathbf{M}_\ell f^{\mu \mathrm{e}} f^{\nu \mathrm{h}}}{E^\lambda - \hbar\omega} \right)$$
$$= \frac{2|\mathbf{A}_0|\omega_q}{\hbar}\,\mathrm{Im}\sum_\lambda \frac{\sum_{\ell'} C_{\ell'}^\lambda \mathbf{M}_{\ell'}^* \sum_\ell C_\ell^{\lambda *}\mathbf{M}_\ell f^{\mu \mathrm{e}} f^{\nu \mathrm{h}}}{E^\lambda - \hbar\omega}. \tag{B.6}$$

Expressing the total dipole matrix elements $\mathbf{M}_\ell$ and the excitonic eigenfunction in terms of the single-particle functions, and including the damping constant γ, we obtain the approximate solution of the photoluminescence intensity.

References

[1] Henini M 2006 *Nanoscale Res. Lett.* **1** 32
[2] Schkolnik A S, Dogonkin E B, Evtikhiev V P, Kotelnikov E Yu, Kudryashov I V, Talalaev V G, Novikov B V, Tomm J W and Gobsch G 2001 *Nanotechnology* **12** 512
[3] Rastelli A, Stufler S, Schliwa A, Songmuang R, Manzano C, Costantini G, Kern K, Zrenner A, Bimberg D and Schmidt O G 2004 *Phys. Rev. Lett.* **92** 166104
[4] Arians R, Kümmell T, Bacher G, Gust A, Kruse C and Hommel D 2007 *Appl. Phys. Lett.* **90** 101114
[5] Kim D, Lefebvre J, Mckee J, Studenikin S, Williams R L, Sachrajda A, Zawadzki P, Hawrylak P, Sheng W, Aers G C and Poole P J 2005 *Appl. Phys. Lett.* **87** 212105
[6] Devreese J T, Fomin V M, Gladilin V N, Pokatilov E P and Klimin S N 2002 *Nanotechnology* **13** 163
[7] Pistone G, Savasta S, Stefano O Di and Girlanda R 2004 *Semicond. Sci. Technol.* **19** S327
[8] Cornet C, Schliwa A, Even J, Doré F, Celebi C, Létoublon A, Macé E, Paranthoën C, Simon A, Koenraad P M, Bertru N, Bimberg D and Loualiche S 2006 *Phys. Rev.* B **74** 035312
[9] Wu H B, Xu S J and Wang J 2006 *Phys. Rev.* B **74** 205329
[10] Zhang Y H, Plaut A S, Harbison J P and Florez L T 2006 *Semicond. Sci. Technol.* **21** 1139
[11] Kira M, Jahnke F and Koch S W 1998 *Phys. Rev. Lett.* **81** 3263
[12] Kira M, Jahnke F, Hoyer W and Koch S W 1999 *Prog. Quantum Electron.* **23** 189
[13] Matsuda K, Saiki T, Saito H and Nishi K 2000 *Appl. Phys. Lett.* **76** 73
[14] Hohenester U, Goldoni G and Molinari E 2004 *Appl. Phys. Lett.* **84** 3963
[15] Koch S W, Meier T, Hoyer W and Kira M 2002 *Physica* E **14** 45
[16] Leosson K, Birkedal D, Magnusdottir I, Langbein W and Hvam J M 2003 *Physica* E **17** 1
[17] Matsuda K, Ikeda K, Saiki T, Tsuchiya H, Saito H and Nishi K 2001 *Phys. Rev.* B **63** 121304(R)
[18] Borri P, Langbein W, Mórk J, Hvam J M, Heinrichsdorff F, Mao M-H and Bimberg D 1999 *Phys. Rev.* B **60** 7784
[19] Uskov A V, Jauho A-P, Tromborg B, Mórk J and Lang R 2000 *Phys. Rev. Lett.* **85** 1516
[20] Kuhn T and Rossi F 1992 *Phys. Rev.* B **46** 7496
[21] Rossi F 1998 *Semicond. Sci. Technol.* **13** 147
[22] Quade W, Schöll E, Rossi F and Jacoboni C 1994 *Phys. Rev.* B **50** 7398
[23] Simserides C, Zora A and Triberis G 2006 *Phys. Rev.* B **73** 155313
[24] Mahan G D 1981 *Many-Particle Physics* (New York: Plenum)
[25] Mauritz O, Goldoni G, Molinari E and Rossi F 2000 *Phys. Rev.* B **62** 8204
[26] Bimberg D, Grundmann M and Ledentsov N N 1999 *Quantum Dot Heterostructures* (New York: Wiley)
Beenakker C W J 1991 *Phys. Rev.* B **44** 1646
[27] Kiravittaya S, Songmuang R, Rastelli A, Heidemeyer H and Schmidt O G 2006 *Nanoscale Res. Lett.* **1** 1
[28] Wimmer M, Nair S V and Shumway J 2006 *Phys. Rev.* B. **73** 165305
[29] Wojs A, Hawrylak P, Fafard S and Jacak L 1996 *Phys. Rev.* B. **54** 5604
[30] Li E H 2000 *Physica* E **5** 215
[31] Hinzer K 2001 Optical properties of GaAs-based self-assembled quantum dots and quantum dot lasers *PhD Thesis* University of Ottawa
[32] Fock V 1928 *Z. Phys.* **47** 446
[33] Darwin C G 1930 *Proc. Camb. Phil. Soc.* **27** 86